Experiments and Simulations on the Nonlinear Control of a Hydraulic Servosystem

Garett A. Sohl and James E. Bobrow, *Member, IEEE*

***Abstract*—This paper presents the derivation, simulation, and implementation of a nonlinear tracking control law for a hydraulic servosystem. An analysis of the nonlinear system equations is used in the derivation of a Lyapunov function that provides for exponentially stable force trajectory tracking. This control law is then extended to provide position tracking. The proposed controller is simulated and then implemented on an experimental hydraulic system to test the limits of its performance and the realistic effects of friction.**

***Index Terms*—Friction compensation, hydraulic force control, hydraulic systems, position control.**

I. Introduction

HYDRAULIC systems are used in a wide variety of industrial applications. These systems provide many advantages over electric motors, including high durability and the ability to produce large forces at high speeds. Unfortunately, the dynamic characteristics of these systems are highly nonlinear and relatively difficult to control. The nonlinearities arise from the compressibility of the hydraulic fluid and the complex flow properties of the servovalve. Friction in the hydraulic cylinder also contributes to the nonlinear behavior [1], [2]. Many current industrial controllers achieve moderate bandwidth with fixed gain controllers by oversizing the cylinder diameter. While a large diameter cylinder increases the effective stiffness of the fluid column in the cylinder, it also requires more costly system components and higher flow rates in order to move at a given speed.

The two most common approaches developed to compensate for the nonlinear behavior of hydraulic servosystems are adaptive control and variable structure control. Most of the adaptive controllers recently developed, such as Huang and Wang [3], Shih and Sheu [4], Kotzev *et al.* [5], and Bobrow and Lum [6] use a linearized model for the system, and hence provide only local stability. These systems have the ability to cope with changing system parameters such as flow constants, fluid bulk modulus, and variable loading. The lack of a global stability proof is often a disadvantage of these linearized adaptive controllers. Given some initial conditions, the adaptive control based on a linearized system model may become unstable.

Manuscript received September 7, 1996; revised February 19, 1998. Recommended by Associate Editor, F. Svaricek. This research was supported by the Parker Hannifin Corporation, Parker Bertea Aerospace Group, and the California Space Institute.

The authors are with the Department of Mechanical and Aerospace Engineering, University of California, Irvine, CA 92697-3975 USA.

Publisher Item Identifier S 1063-6536(99)01799-6.

An alternative to adaptive control is variable structure control (VSC). Several versions of these sliding mode controllers have been developed for hydraulic systems [7]–[9]. These VSC approaches are robust to large parameter variations and are globally stable. However, an important practical problem is the selection and tuning of the required dead band. If one selects too small a dead band, the nearly discontinuous control excites unmodeled dynamics present in the system. If the dead band is too large, a degradation tracking performance occurs.

In our approach, the controller is derived from a Lyapunov analysis of the nonlinear dynamic equations for the servovalve and hydraulic cylinder. The basic form of control law obtained is similar to those developed by Vossoughi and Donath [10], Alleyne [11], Del Re and Isidori [12] and Hahn *et al.* [13]. In [10], [12] and [13], the nonlinear control is obtained from a feedback linearization framework. This perspective has the advantage that the linearized system can use well established tools from robust control theory to enhance the robustness of the linearized system [10]. Our Lyapunov-based approach separates the force control subsystem from the position tracking subsystem using a technique similar to integrator backstepping [14]. The same basic idea has been used for force control [11]. The experimental tests demonstrate that the fluid bulk modulus and valve flow parameters are important for successful control and we give a method for the off-line identification of these parameters. We also show that for a real system, friction can have a large effect on tracking accuracy, but this effect can be compensated for fairly accurately.

II. System Model

Fig. 1 presents an overview of the hydraulic system considered in this paper. The analysis of hydraulic servosystems of this type is well documented in the literature [15].

A. Servovalve

Since our maximum closed-loop system bandwidth is roughly 10 Hz, we assume that the control u applied to the spool valve is directly proportional to the spool position, i.e., the dynamics of the valve motor/flapper are fast enough to be neglected. The effects of servovalve dynamics have been included by other researchers [11] but this requires an additional sensor to obtain the spool position and only minimal performance improvement is achieved for position tracking. Neglecting leakage in the valve, the flow into sides 1 and 2

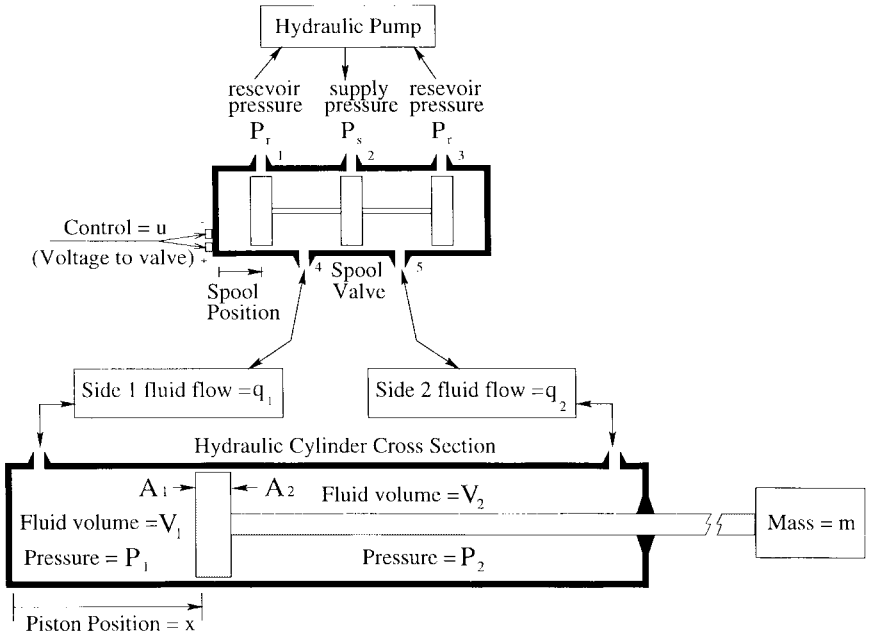

Fig. 1. Overview of hydraulic system.

of the cylinder is

$$q_1 = \begin{cases} c_1 u \sqrt{p_s - p_1}, & \text{for } u \geq 0 \\ c_2 u \sqrt{p_1 - p_r}, & \text{for } u < 0 \end{cases} \tag{1}$$

and

$$q_2 = \begin{cases} -c_3 u \sqrt{p_2 - p_r}, & \text{for } u \geq 0 \\ -c_4 u \sqrt{p_s - p_2}, & \text{for } u < 0 \end{cases} \tag{2}$$

where p_s is the supply pressure, p_r is the reservoir pressure, p_1 and p_2 are the pressure guage values, above one atmosphere, on the two cylinder sides and c_1, c_2, c_3 and c_4 are the valve orifice coefficients. These coefficients are determined by the shape and size of the valve orifices. Values for these coefficients are often provided by the manufacturer but more accurate values can be obtained using off-line testing.

B. Compressibility

Hydraulic fluid compressibility is governed by the equation, $\beta = -V(dp/dv)$, where β is the fluid bulk modulus and V is the chamber volume. Applying this to the two sides of the cylinder yields

$$\dot{p}_1 = \frac{\beta}{V_1}(-\dot{V}_1 + q_1) \tag{3}$$

$$\dot{p}_2 = \frac{\beta}{V_2}(-\dot{V}_2 + q_2) \tag{4}$$

where $V_1 = V_{10} + xA_1$ and $V_2 = V_{20} + (s - x)A_2$ are the total fluid volumes in the two sides of the cylinder, s is the cylinder stroke, x is the piston position and V_{10} and V_{20} are the volumes of fluid in the lines and fittings on the two sides of the cylinder. An empirical value for the fluid bulk modulus is determined from an off-line system investigation described in Section V.

C. Piston Motion

Differentiating the fluid force on the piston yields

$$\dot{F} = \dot{p}_1 A_1 - \dot{p}_2 A_2. \tag{5}$$

After substituting our expressions for $\dot{p}_1$ and $\dot{p}_2$ from (3) and (4) and realizing that $\dot{V}_1 = A_1\dot{x}$ and $\dot{V}_2 = -A_2\dot{x}$ we have

$$\dot{F} = -\dot{x}\beta\left(\frac{A_2^2}{V_2} + \frac{A_1^2}{V_1}\right) + z(x, p_1, p_2)u \tag{6}$$

where

$$z = \begin{cases} \beta\left(\dfrac{A_2 c_3}{V_2}\sqrt{p_2 - p_r} + \dfrac{A_1 c_1}{V_1}\sqrt{p_s - p_1}\right) & u \geq 0 \\ \beta\left(\dfrac{A_2 c_4}{V_2}\sqrt{p_s - p_2} + \dfrac{A_1 c_2}{V_1}\sqrt{p_1 - p_r}\right) & u < 0 \end{cases} \tag{7}$$

Equations (6) and (7) are useful since the control u appears explicitly in them. This allows one to choose $\dot{F}$ by adjusting the control input u. As shown in the next section, the problem of choosing a control input is therefore reduced to the problem of determining a good choice for $\dot{F}$.

III. Control Law Analysis

We will begin the derivation of the control law with the choice of a 'Lyapunov like' function,

$$V(\boldsymbol{x}, t) = \tfrac{1}{2}\, k_L (F - F_d)^2 \tag{8}$$

where F is the net force of the hydraulic fluid on the piston, F_d is the desired force and $\boldsymbol{x}$ is the state vector, $(x, \dot{x}, p_1, p_2)$. The desired force, F_d, in (8) is assumed to be a C^1 differentiable function.

$V(\boldsymbol{x}, t)$ in (8) is not a true Lyapunov function since it is not a positive definite function of the the four states. In order to use this function for the stability proof we first note that

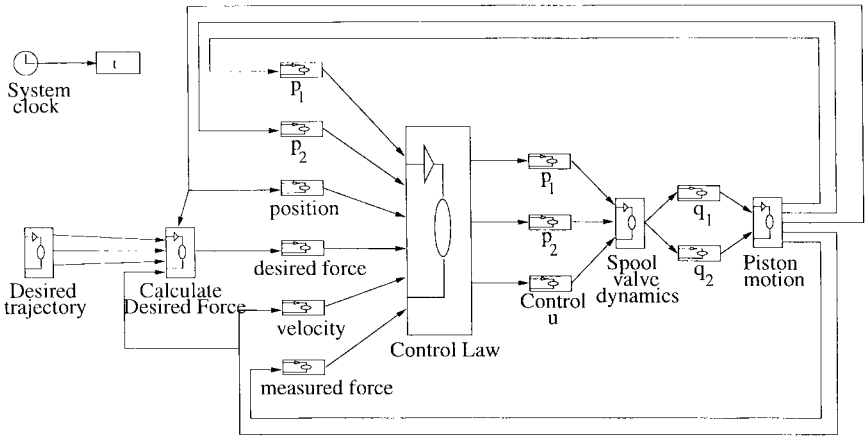

Fig. 2. Simulation block diagram.

$V(\boldsymbol{x},t)$ is lower bounded by zero. Taking the derivative of $V(\boldsymbol{x},t)$ we have

$$\dot{V}(\boldsymbol{x},t) = k_L(F - F_d)(\dot{F} - \dot{F}_d). \tag{9}$$

If we choose u such that

$$u = \frac{1}{z}\left(\dot{F}_d - k_F(F - F_d) + \dot{x}\beta\left(\frac{A_2^2}{V_2} + \frac{A_1^2}{V_1}\right)\right) \tag{10}$$

where k_F is a positive force error gain and the nonzero quantity z is defined in (7), we see that $\dot{F}$ in (6) becomes

$$\dot{F} = \dot{F}_d - k_F(F - F_d). \tag{11}$$

This guarantees exponential force stabilization with

$$(F - F_d) = \hat{e}^{k_F t}(F(0) - F_d(0)) \tag{12}$$

Note that (12) shows that $(F(t) - F_d(t)) \to 0$ with time constant $\tau = 1/k_f$. This can also be shown as a result of Barbalat's Lemma. Substituting the expression for $(\dot{F} - \dot{F}_d)$ from (11) into (9) we have

$$\dot{V}(\boldsymbol{x},t) = -k_L k_F(F - F_d)^2 = -2k_F V \tag{13}$$

Therefore, $\dot{V}(\boldsymbol{x},t)$ is negative semidefinite.

Finally, note that if $\dot{V}(\boldsymbol{x},t)$ is uniformly continuous in time then Barbalat's Lemma [16] states that $\dot{V}(\boldsymbol{x},t) \to 0$ as $t \to \infty$. A sufficient condition for this final criteria is for $\ddot{V}(\boldsymbol{x},t)$ to be bounded. Taking the derivative of $\dot{V}(\boldsymbol{x},t)$ we have

$$\ddot{V}(\boldsymbol{x},t) = -2k_L k_F(F - F_d)(\dot{F} - \dot{F}_d) \tag{14}$$

Our choice of u in (10) gives $(\dot{F} - \dot{F}_d) = -k_F(F - F_d)$ so therefore

$$\ddot{V}(\boldsymbol{x},t) = 2k_L k_F^2(F - F_d)^2 = 4k_F^2 V(\boldsymbol{x},t). \tag{15}$$

This shows that $\ddot{V}(\boldsymbol{x},t)$ is bounded and therefore Barbalat's Lemma tells us $(F(t) - F_d(t)) \to 0$ as $t \to \infty$ with the control law given in (40).

A. Position Tracking

In order to achieve position tracking, we choose the desired force to be

$$F_d = m\ddot{x}_d(t) - k_v(\dot{x}(t) - \dot{x}_d(t)) - k_p(x(t) - x_d(t)) + \hat{g}(\dot{x}) \tag{16}$$

where $\hat{g}(\dot{x})$ is an estimate of the friction forces in the cylinder. Recall that we chose F to represent only the fluid force $(p_1A_1 - p_2A_2)$ on the piston; the total force on the piston includes friction, so the equation of motion is given by

$$F - g(\dot{x}) = m\ddot{x} \tag{17}$$

where m is the total mass being moved and $g(\dot{x})$ is the force of Coulomb friction and stiction. Subtracting (16) from (17) and letting $e = x - x_d$ yields

$$m\ddot{e} + k_v\dot{e} + k_p e = (F - F_d) + \delta(\dot{x}) \tag{18}$$

where $\delta(\dot{x}) = \hat{g}(\dot{x}) - g(\dot{x})$ can be considered a disturbance due to inaccurate friction modeling. Equation (18) is a second-order linear system in e driven by $(F - F_d)$ and $\delta(\dot{x})$. The disturbance δ is bounded and $(F - F_d) \to 0$, so (18) is a stable system. If we have perfect knowledge of the cylinder friction (i.e., $\delta = 0$), (18) guarantees that $e \to 0$. For bounded initial conditions and a constant δ, we see that $|e| \leq (1/k_p)|\delta|$ at steady state. For time varying $\delta(\dot{x})$, (18) can be thought of as a second-order low-pass filter driven by the disturbance $\delta(\dot{x})$.

IV. Simulation

The proposed control law was simulated using Matlab's simulink package. Fig. 2 presents the general block diagram for the simulated control system. The simulated system consists of four main parts. First, the desired trajectory information is used to determine the desired force as described in (16). Equation (10) is then used to determine the control signal. This signal is sent to the simulated spool valve which uses (1) and (2) to obtain the flow rates q_1 and q_2. Equations (3) and (4) are then used by the simulation to determine the motion of the piston and yield the new system states ($x, \dot{x}, p_1$ and p_2).

Several simulations were performed with various input trajectories to determine the controller's position tracking

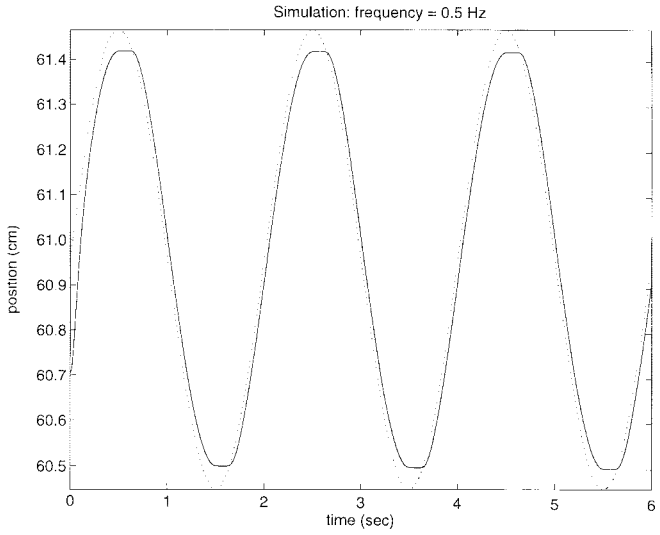

Fig. 3. Simulated position tracking, $\hat{g} = 0$.

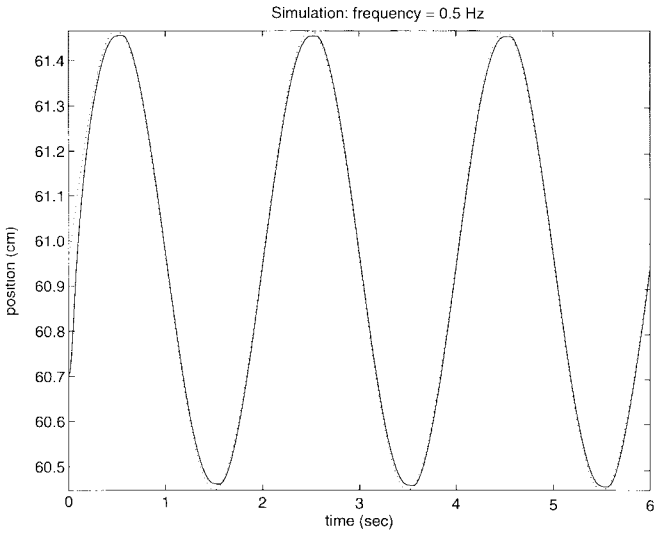

Fig. 4. Simulated position tracking, $\hat{g} = 75\%$ of actual friction.

characteristics. As expected, the simulated system tracks the desired trajectory with little or no error when the controller is given perfect knowledge of the system.

The simulation was also used to examine the effects of errors in the system parameters. These parameters include the valve coefficients, system mass, fluid bulk modulus, and friction terms. The introduction of errors in these parameters reduces tracking performance. The system is most sensitive to errors in the valve coefficients and friction terms. Errors in the other parameters only become significant at high speeds. As we noted in (18), errors in friction modeling enter as a disturbance in the position tracking dynamics. The effects of different friction models was also examined in simulation. Figs. 3 and 4 show the performance increase obtained by more accurate friction modeling.

V. Controller Implementation

After achieving acceptable performance in simulation, the control law was implemented on the existing hydraulic test system shown in Fig. 5. The test cylinder has a 1.22-m stroke and a 5.1-cm diameter. The piston was connected to 454-kg of weights mounted on a horizontal linear track. Fluid pressure was supplied at 6895 kPa by a Parker–Hannifin hydraulic pump. A 16 bit MetroByte A/D and D/A board connected to an IBM compatible personal computer was used to obtain system data from the two pressure transducers and output the control signal to the servovalve. A sampling rate of 500 Hz was used.

A. Parameter Identification

The control law of (10) requires estimates of the valve coefficients and fluid bulk modulus. Values for the valve coefficients are often provided by the manufacturer of the servovalve, but since the simulation identified these parameters as the most critical they should be checked for accuracy. The fluid bulk modulus can vary significantly with temperature and should also be verified.

A least squares analysis of the data obtained from several open-loop tests was used to obtain experimental values for the valve coefficients and the fluid bulk modulus. The control input for these tests consisted of various sine sweeps. The system state $(x, \dot{x}, p_1, p_2)$ was recorded at 500 Hz during these tests. The test data provides us with values for V_1, V_2, p_1, p_2 and x for each of the sampled data points taken during one test. We then use finite difference derivatives to obtain values for $\dot{p}_1, \dot{p}_2$, and $\dot{x}$.

In order to use a least squares analysis of this data, we first need to cast the data in the form $D\boldsymbol{x} = b$ where $D \in \Re^{mxn}$ and $b \in \Re^m$ are known, $\boldsymbol{x} \in \Re^n$ is unknown and $m \gg n$. Substituting the expression for the flow rates from (1) and (2) into (3) and (4) we can derive equations of the form

$$\begin{pmatrix} -\dot{p}_1(1)V_1 & w_1(1) & w_2(1) \\ -\dot{p}_1(2)V_1 & w_1(2) & w_2(2) \\ \vdots & \vdots & \vdots \\ -\dot{p}_1(n)V_1 & w_1(n) & w_2(n) \end{pmatrix} \begin{pmatrix} \frac{1}{\beta} \\ c_1 \\ c_2 \end{pmatrix} = \begin{pmatrix} A_1\ddot{x}(1) \\ A_1\ddot{x}(2) \\ \vdots \\ A_1\ddot{x}(n) \end{pmatrix} \tag{19}$$

where (for $T = 1, 2, \cdots, n$)

$$\left.\begin{aligned} w_1(T) &= u(T)\sqrt{p_s - p_1(T)} \\ w_2(T) &= 0 \end{aligned}\right\}, \qquad \text{for} \quad u(T) \geq 0 \tag{20}$$

and

$$\left.\begin{aligned} w_1(T) &= 0 \\ w_2(T) &= u(T)\sqrt{p_1(T) - p_r} \end{aligned}\right\}, \qquad \text{for} \quad u(T) < 0. \tag{21}$$

A similar equation is also derived for unknowns c_3 and c_4. In Matlab, the command $\boldsymbol{x} = D\backslash b$ was used to solve these equations for values of β, c_1, c_2 and c_3 that minimize $\|D\boldsymbol{x} - b\|^2$. Values from several test runs were averaged together in order to achieve good parameter estimates.

VI. Friction Model

Friction in the hydraulic cylinder has a significant effect on the controller's performance as predicted by the simulation.

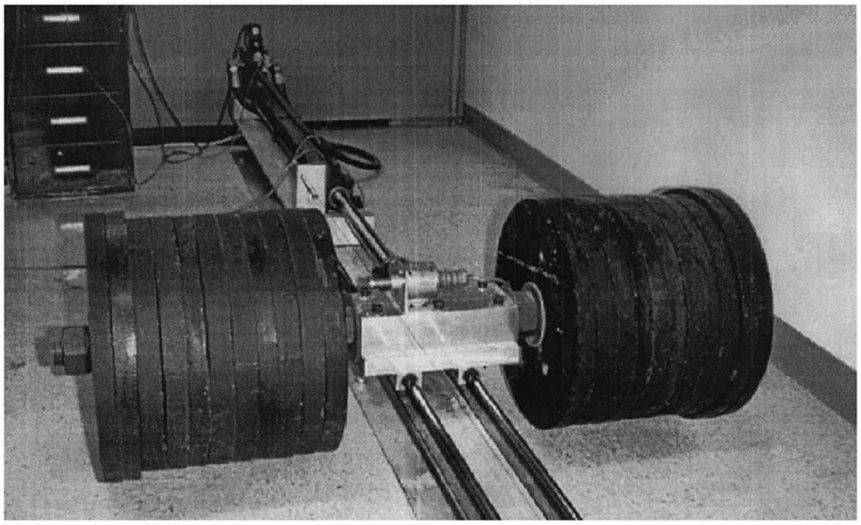

Fig. 5. Hydraulic test system.

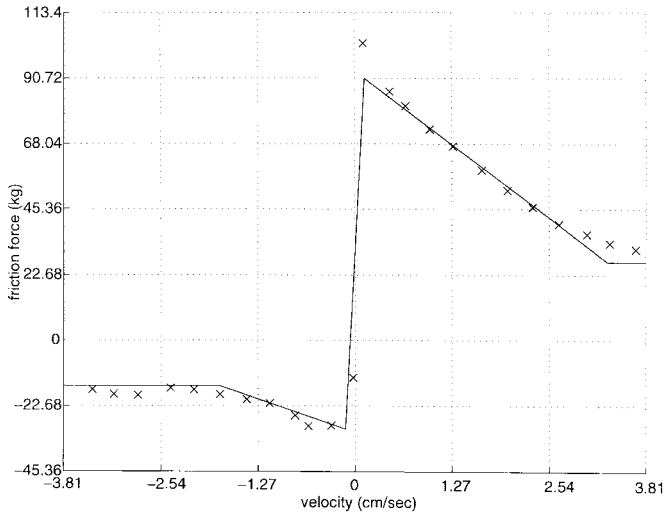

Fig. 6. Observed friction force versus piston velocity.

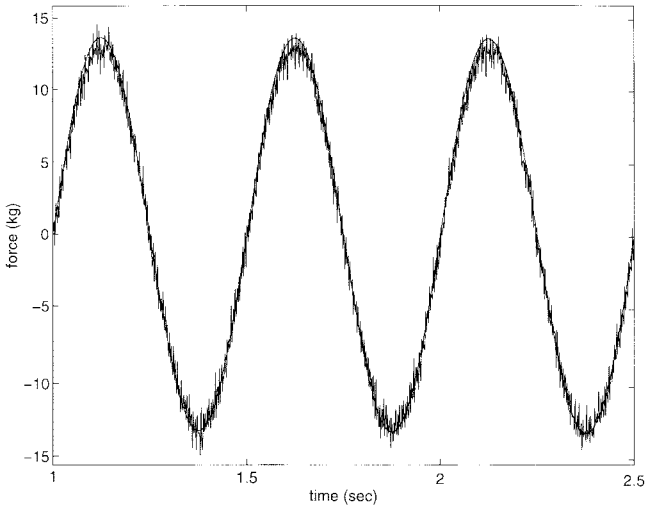

Fig. 7. Force tracking: 2 Hz.

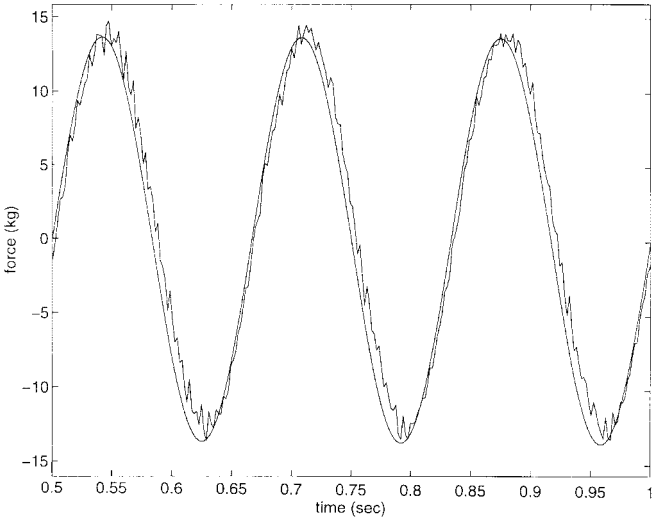

Fig. 8. Force tracking: 6 Hz.

One standard expermental method is to model friction as a function of velocity [17], [18]. By measuring the friction force required to move the piston at a constant velocity, we can develop such a model for $g(\dot{x})$. A simple open-loop constant control signal was used to move the cylinder and record the friction data. Averages of several tests are shown as data points in Fig. 6. At high speeds ($|\dot{x}| > 3.8$ cm/s) Coulomb friction is dominant and the friction force is fairly constant. Stiction dramatically increases the friction at low speeds, especially when moving in the positive direction. In the implementation of our controller, the simple piecewise continuous linear function shown in Fig. 6 was used to model friction as a function of piston velocity, $\hat{g}(\dot{x})$.

VII. Force Tracking

Given estimates for the valve parameters and fluid bulk modulus, the control law of (10) was used to track a desired force. The stability analysis presented earlier shows that $F \rightarrow F_d$ as $t \rightarrow \infty$. Results for tracking sinusoidal force trajectories are shown in Figs. 7–10. The forces used in these tests are smaller than the static friction of the piston and allow the piston to remain stationary. The extra high-frequency dynamics in these plots is caused by standing pressure waves

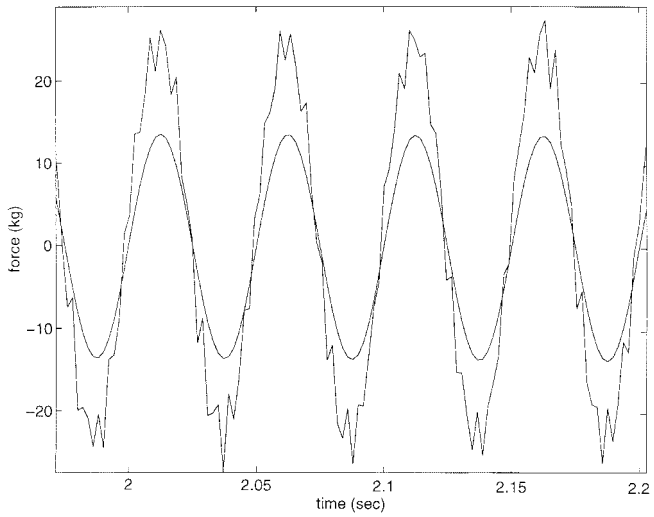

Fig. 9. Force tracking: 20 Hz.

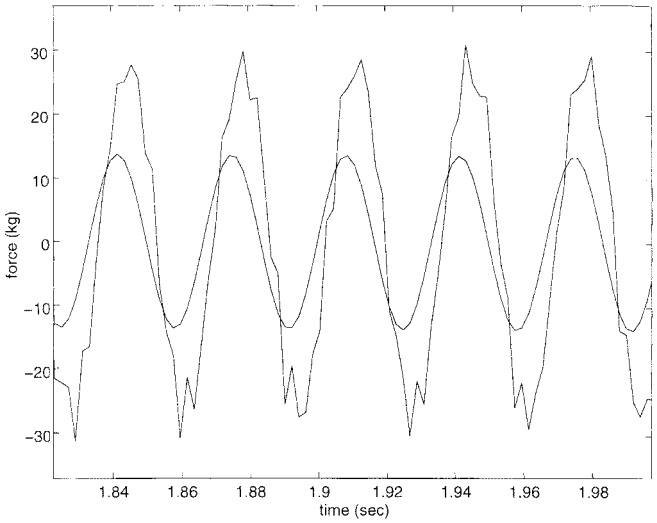

Fig. 10. Force tracking: 30 Hz.

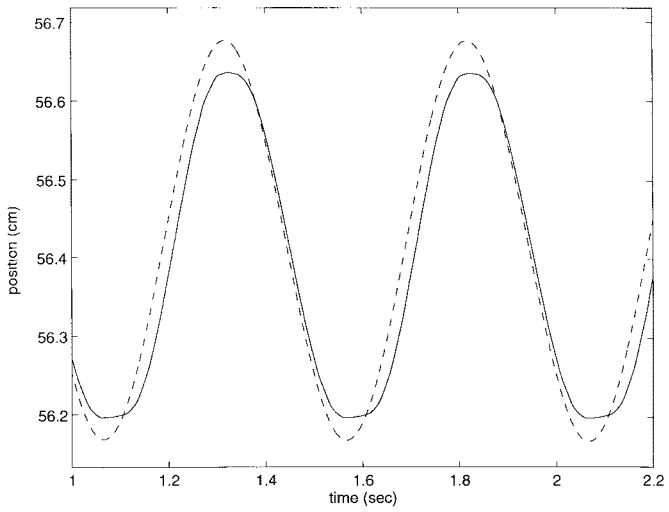

Fig. 11. Proposed controller: 2 Hz, no friction estimate used.

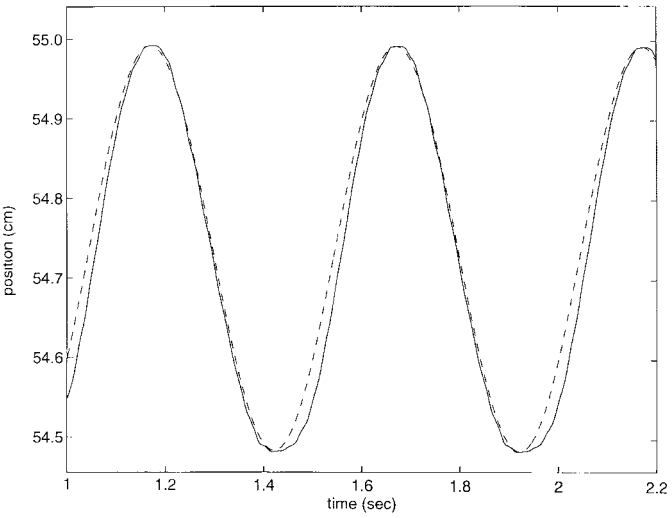

Fig. 12. Proposed controller: 2 Hz, constant Coulomb friction only.

in the hydraulic lines which occur at approximately 195 Hz. We believe tracking error increased at higher frequencies due to our assumption that the valve dynamics are negligible.

VIII. Position Tracking

Having shown that the system can track a desired force, we now let $F_d = m\ddot{x}_d - k_v(\dot{x} - \dot{x}_d) - k_p(x - x_d) + \hat{g}(\dot{x})$ where $\hat{g}(\dot{x})$ is the estimate of the friction in the cylinder. This choice for F_d allows us to track a desired position trajectory, $x_d(t)$. The bandwidth and step response of the proposed controller can then be compared to traditional P and PD controllers.

A. Friction Estimates

As we saw in Fig. 6, friction forces in the cylinder can be quite high. These forces must be modeled correctly in order to achieve good tracking performance [see (18)]. Fig. 11 shows the poor performance of our controller when cylinder friction is neglected. This closely matches the simulation results in Fig. 3. The addition of a constant Coulomb friction term to the control law greatly improves the tracking performance as shown in Fig. 12, but does not work well for low positive velocities where the friction force is highest. Using the piecewise linear friction estimate $\hat{g}(\dot{x})$ shown in Fig. 6 we can improve the performance in the low speed regions as shown in Fig. 13.

B. Bandwidth

Bandwidth tests were performed in order to determine the maximum frequency the controller could accurately track a given amplitude. In order to establish a baseline for comparison purposes, we first ran experiments using well-tuned P and PD controllers. Fig. 14 shows the response of a simple proportional controller (i.e., $u = -k_P(x - x_d)$) while tracking a 0.51 cm sine wave at 2 Hz. To find k_p for this controller, we used a standard tuning procedure [19]. That is, k_p was increased on the experimental system until an oscillatory response was observed. The instability occurs first near the ends of the cylinder since the nonlinear term z in (6) is largest at the cylinder ends. Because the gain k_p is a *constant*,

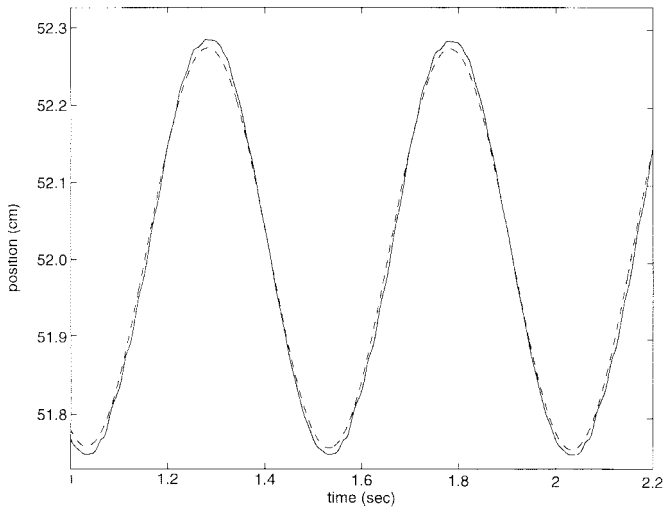

Fig. 13. Proposed controller: 2 Hz, piecewise linear friction estimate of Fig. 6.

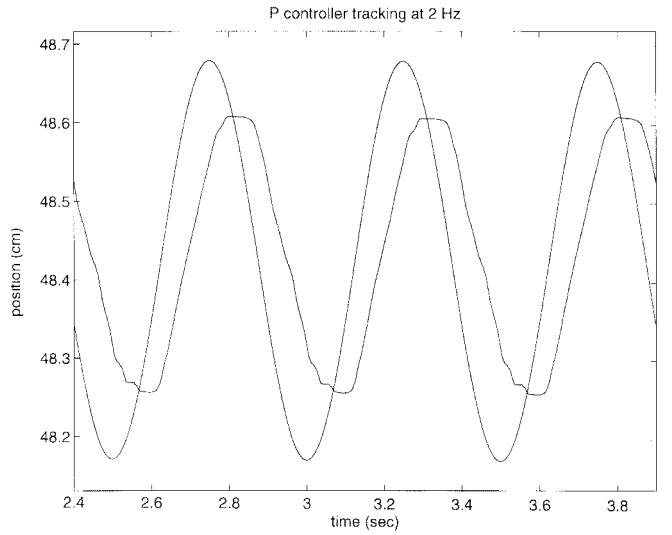

Fig. 14. P controller: 2 Hz.

the value that works well at the cylinder ends was used for all cylinder postitions. A similar procedure was used to find the derivative term in a PD control law. Fig. 15 shows the bandwidth response of a PD controller with $u = -k_P(x - x_d) - k_v(\dot{x} - \dot{x}_d)$. The addition of the derivative term does little to increase the performance due to the large amount of damping provided by friction.

Given the relatively poor response of the system using the PD control law, it would be desirable to improve the performance using friction compensation and modern control. Friction compensation is difficult since the control u drives the *derivative* of the actuator force through (6) so one can not directly cancel the friction term as is commonly done with electric motors. Advanced linear control theory also does little to improve the performance of this system since the strong nonlinearities in the system dynamics require some form of variable feedback gains to obtain good performance. In contrast, our nonlinear control approach overcomes these limitations.

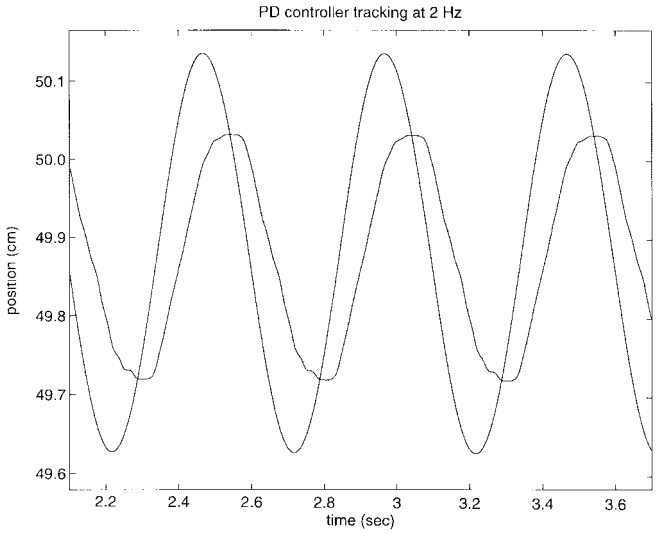

Fig. 15. PD controller: 2 Hz.

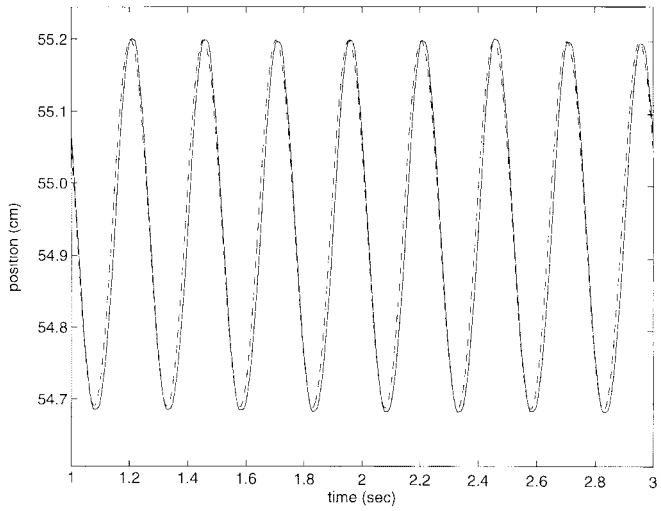

Fig. 16. Proposed controller: 4 Hz.

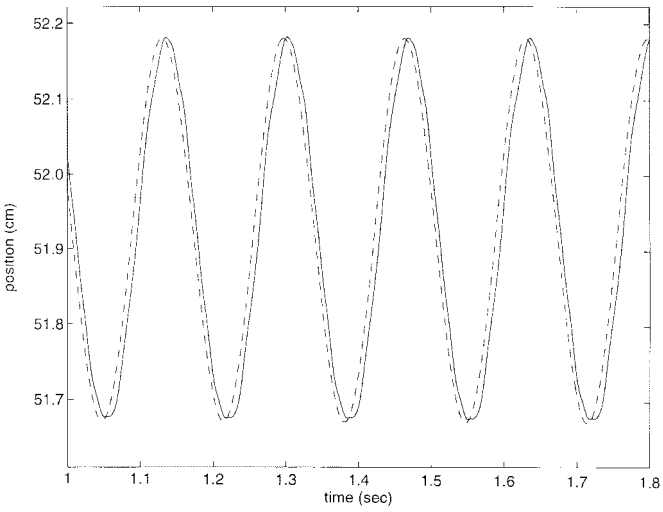

Fig. 17. Proposed controller: 6 Hz.

Figs. 13, and 16–19 show the tracking of our controller at 2, 4, 6, 8.5, and 11.5 Hz. Even at high frequencies, the proposed controller has only a small phase shift. The

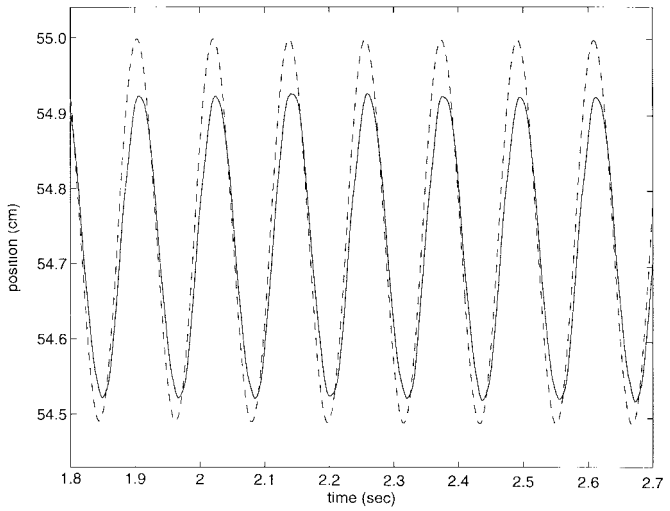

Fig. 18. Proposed controller: 8.5 Hz.

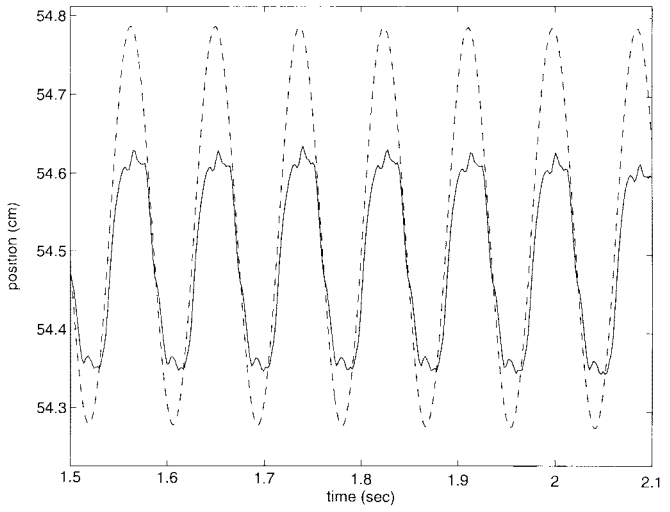

Fig. 19. Proposed controller: 11.5 Hz.

controller's performance does begin to degrade at frequencies over 8 Hz, where it fails to reach the desired peak amplitude.

C. Step Response

Step response tests identify several important characteristics of a controller, including speed of response, overshoot, settling time and steady state error. For our tests a 7th order polynomial is used to generate a smooth step function and provide continuous velocity and acceleration trajectories.

Figs. 20 and 21 show the step response of a simple proportional controller. The settling time of the proportional controller is approximately 0.4 s. Figs. 22 and 23 show the step response of the proposed controller for the same step functions used in the previous tests. This controller provides much faster settling times (approximately 0.14 seconds) when compared to the P controller. Response time is quicker due to more accurate friction modeling.

D. Path Tracking

The bandwidth and step response tests performed on the system considered only small amplitude motions near the

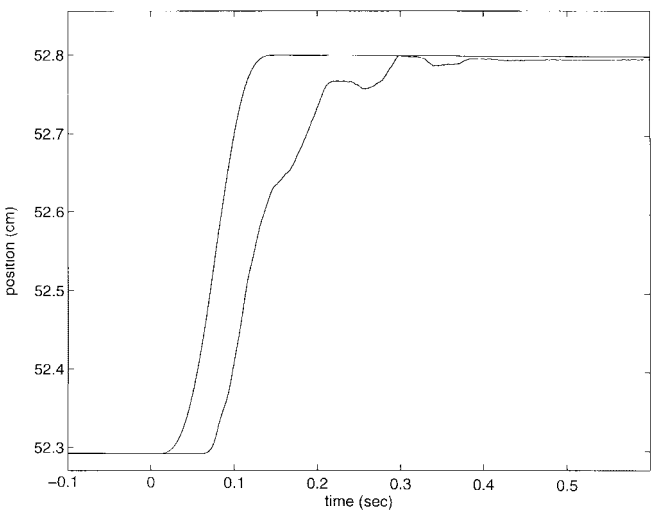

Fig. 20. Proportional controller smooth step response with a rise time of 0.15 s.

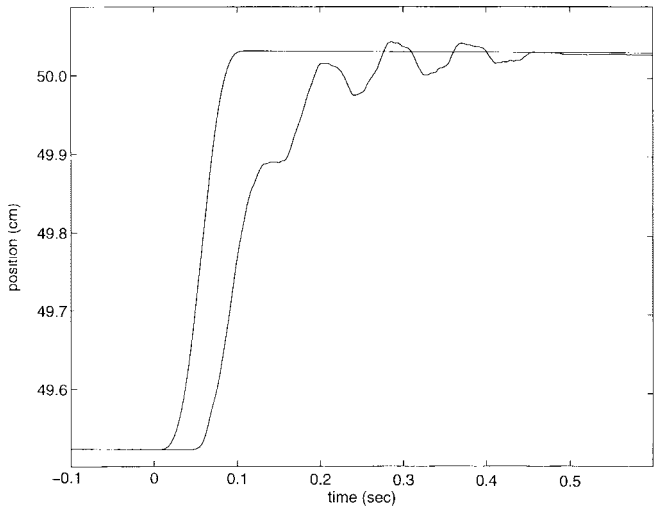

Fig. 21. Proportional controller smooth step response with a rise time of 0.11 s.

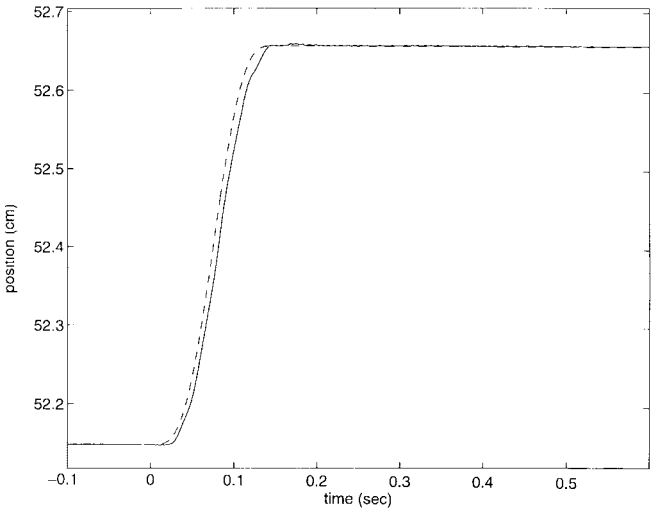

Fig. 22. Smooth step response with a rise time 0.15 s.

cylinder mid-stroke position. To show the performance of the controller throughout the cylinder stroke, a large amplitude

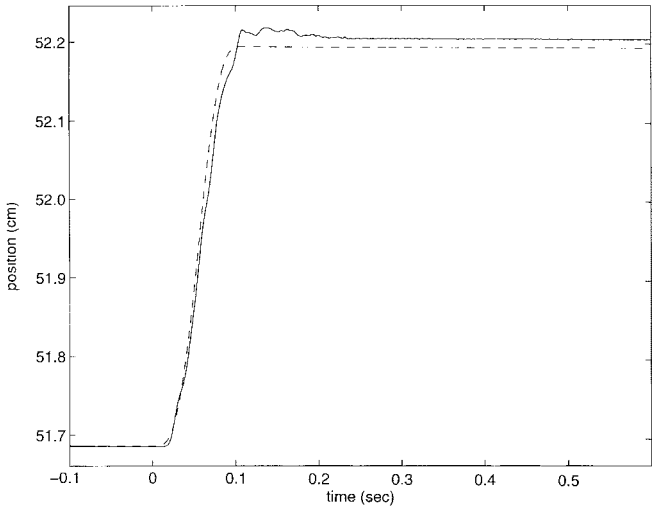

Fig. 23. Smooth step response with a rise time of 0.11 s.

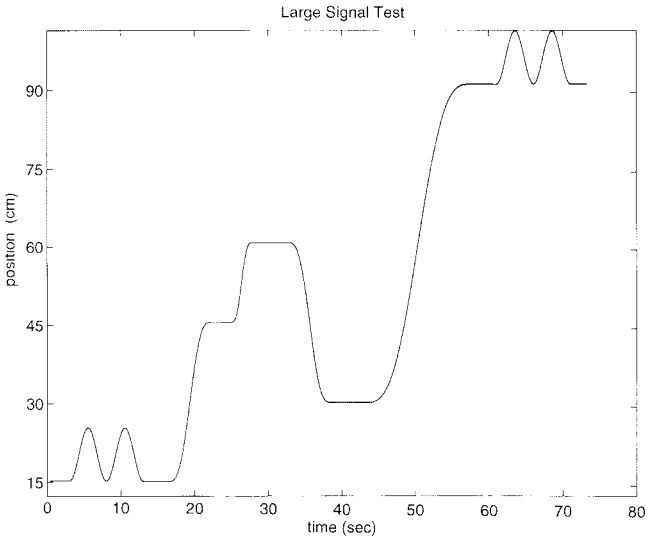

Fig. 24. Desired path for path tracking tests.

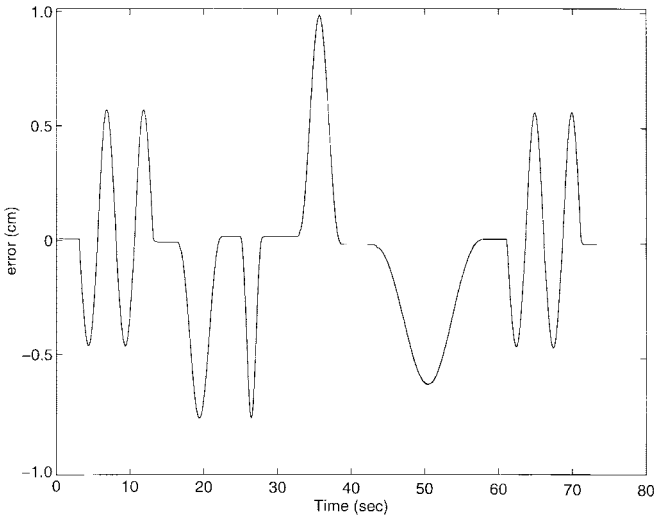

Fig. 25. P controller.

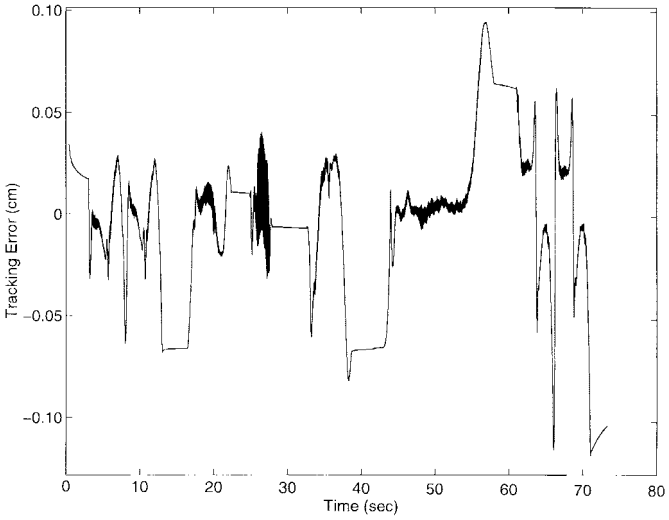

Fig. 26. Proposed controller.

path, shown in Fig. 24, which provided motion throughout the range of the cylinder stroke, was used. This test exercised the nonlinear features of the proposed control law. Fig. 25 shows the position error of a proportional controller while attempting to follow this path. Fig. 26 shows the performance of our controller while tracking the same path. The peak tracking error for our controller is only 10% of the error observed for the proportional controller.

IX. Conclusions

In this paper we have presented the derivation, simulation, and implementation of a nonlinear control law for hydraulic servosystems. The proposed controller provides exponential stability for force tracking. Position tracking is also possible provided an accurate friction model is developed. The simulation of the controller demonstrates good position tracking even in the presence of errors in the physical parameters. Applying the controller to an existing experimental hydraulic system provided excellent force and position tracking without the complexity of variable structure or adaptive methods.

References

[1] C. Canudas de Wit, H. Olsson, K. J. Astrom, and P. Lischinsky, "A new model for control of systems with friction," *IEEE Trans. Automat. Contr.*, vol. 40, pp. 419–425, Mar. 1995.

[2] M'Sirdi Nacer Laurent Laval and Cadiou Jean-Charles, "h_∞ force control of a hydraulic servo-actuator with environmental uncertainties," in *Proc. 1996 IEEE Conf. Robot. Automat.*, Minneapolis, MN, Apr. 1996, pp. 1566–1571, IEEE.

[3] C. H. Huang and Y. T. Wang, "Self-optimization adaptive velocity control of asymmetric hydraulic actuator," *Int. J. Adaptive Contr. Signal Processing*, vol. 9, no. 3, pp. 271–283, May–June 1995.

[4] M.-C. Shih and Y.-R. Sheu, "The adaptive position control of an electro hydraulic servo cylinder," *JSME Int. J.*, vol. 34, no. 3, pp. 370–376, 1991.

[5] A> Kotzev, D. B. Cherchas, and P. D. Lawrench, "Performance of generalized predictive control with on-line model order determination for a hydraulic robotic manipulator," *Robotics*, vol. 13, pp. 55–64, Jan.–Feb. 1994.

[6] J. E. Bobrow and K. Lum, "Adaptive, high bandwidth control of a hydraulic actuator," in *Proc. 1995 Amer. Contr. Conf.* Evanston, IL: Amer. Automat. Contr. Council, June 1995, pp. 71–75.

[7] T. L. Chern and Y. C. Wu, "Design of integral variable structure controller and application to electrohydraulic velocity servosystems," *Proc. Inst. Electr. Eng.*, pt. D (Control Theory and Applications), vol. 138, no. 5, pp. 439–444, Sept. 1991.
[8] K.-I. Lee and D.-K. Lee, "Tracking control of a single-rod hydraulic cylinder using sliding mode," in *Proc. 29th SICE Annu. Conf.*, Tokyo, Japan, July 1990, pp. 865–868.
[9] C. L. Hwang and C. H. Lan, "The position control of electrohydraulic servomechanism via a novel variable structure control," *Mechatronics*, vol. 4, no. 4, pp. 369–391, June 1994.
[10] M. Donath and R. Vossoughi, "Dynamic feedback linearization for electrohydraulically actuated servosystems," in *Proc. 1992 Japan/USA Symp. Flexible Automat.*, San Francisco, CA, July 1992, pp. 595–606.
[11] A. Alleyne, "Nonlinear force control of an electro-hydraulic actuator," in *Proc. 1996 Japan/USA Symp. Flexible Automat.*, Boston, MA, 1996.
[12] L. Del Re and A. Isidori, "Performance enhancement of nonlinder drives by feedback linearization of linear-bilinear cascade models," *IEEE Trans. Contr. Syst. Technol.*, vol. 3, pp. 299–308, 1995.
[13] H. Hahn, A. Piepenbrink, and K. D. Leimbach, "Input/output linearization control of an electro servo-hydraulic actuator," in *Proc. 3rd IEEE Conf. Contr. Applicat.*, Glasgow, U.K., Aug. 1994, pp. 995–1000, IEEE.
[14] P. Kokotovic, "The joy of feedback: Nonlinear and adaptive," *IEEE Contr. Syst.*, vol. 12, no. 3, pp. 7–17, June 1992.
[15] H. E. Merrit, *Hydraulic Control Systems*. New York: Wiley, 1976.
[16] J.-J. Slotine and W. Li, *Applied Nonlinear Control*. Englewood Cliffs, NJ: Prentice-Hall, 1991.
[17] C. T. Johnson and R. D. Lorenz, "Experimental identification of friction and its compensation in precise, position controlled mechanisms," *IEEE Trans. Ind. Applicat.*, vol. 28, pp. 1392–1398, Nov.–Dec. 1992.
[18] C. Canudas de Wit, P. Noel, A. Aubin, and B. Brogliato, "Adaptive friction compensation in robot manipulators: Low-velocities," *Int. J. Robot. Res.*, no. 3, pp. 189–199, June 1991.
[19] J. Johnson, *Design of Electrohydraulic Systems for Industrial Motion Control*. Irvine, CA: Parker Hannifin, 1991.

Garett A. Sohl received the B.S. degree in mechanical engineering in 1993 from Rice University, Houston, TX, and the M.S. degree from the University of California, Irvine in 1996. He is a Ph.D. student in Mechanical and Aerospace Engineering at the University of California, Irvine.

He received the Parker Hannifin graduate research fellowship in 1993 to support his M.S. research in hydraulic control system design. He is currently working on computational dynamics for biomimetic robots.

James E. Bobrow (M'85) received the M.S. and Ph.D. degrees in engineering from the Mechanics and Structures Department of the University of California, Los Angeles, in 1983. His Ph.D. thesis was on the optimal control of robotic manipulators.

He is a Professor of Mechanical and Aerospace Engineering at the University of California, Irvine. After graduate school, he was a senior Programmer Analyst at McDonnell Douglas Automation Company, where he developed CAM software for the Unigraphics system. In July 1984, he joined UCI as an Assistant Professor, where he conducted research in robotics and applied control systems. In the 1991–1992 academic year, he was a Visiting Associate Professor in the Computer Science Department at Stanford University, where he investigated applications of numerical optimization algorithms to learning systems. He has published over 60 research papers in robotics, applied control systems, numerical optimization techniques, and computer-aided design.